REPORT DOCUMENTATION PAGE

Form Approved
OMB NO. 0704-0188

1. AGENCY USE ONLY (Leave Blank)	2. REPORT DATE	3. REPORT TYPE AND DATES COVERED
	June 12, 2009	Final Report,

4. TITLE AND SUBTITLE
New Electrocatalysts for Direct Oxidation of Organic Fuels

5. FUNDING NUMBERS
[redacted]
ARO_MI-PR

6. AUTHOR(S)
Elton J. Cairns and Jeffrey A. Reimer

7. PERFORMING ORGANIZATION NAME(S) AND ADDRESS(ES)
Lawrence Berkeley National Laboratory
Berkeley, CA 94720

8. PERFORMING ORGANIZATION REPORT NUMBER

9. SPONSORING / MONITORING AGENCY NAME(S) AND ADDRESS(ES)
U. S. Army Research Office
P.O. Box 12211
Research Triangle Park, NC 27709-2211

10. SPONSORING / MONITORING AGENCY REPORT NUMBER
48713.1-CH

11. SUPPLEMENTARY NOTES
The views, opinions and/or findings contained in this report are those of the author(s) and should not be construed as an official Department of the Army position, policy or decision, unless so designated by other documentation.

12 a. DISTRIBUTION / AVAILABILITY STATEMENT
Approved for public release; distribution unlimited.

12 b. DISTRIBUTION CODE

13. ABSTRACT (Maximum 200 words)
This project has fosused on a detailed study of electrocatalysis of organic fuels and important intermediates (CO_{ads}) on platimun and platinum alloy electrocatalysts, using advanced NMR tools developed in our laboratory. The highlights of the results include:

- CO(g) and CH_3OH adsorb onto and are oxidized from two types of Pt sites: weakly-bound (WB) hydrogen closely-packed (110-like) sites, and strongly-bound (SB) hydrogen loosely-packed (100-like) sites.
- Relative rates of adsorption have been measured for CO(g) and CH_3OH on the two types of Pt sites.
- The CV for CO_{ads} oxidation has been modeled and deconvoluted, and CO_{ads} oxidation rate constants have been measured for various surface coverages.
- The $^{13}CO_{ads}$ NMR results are consistent with the two-site model. The NMR peak shift quantitatively indicates the relative occupancy of the two types of sites.
- The $^{13}CO_{ads}$ NMR peak shape and relaxation times are consistent with a two-site exchange model for CO_{ads} mobility on Pt surfaces. The exchange rate constant has been measured, and the frequency difference for the ^{13}CO NMR lines corresponding to the two types of sites has been determined.

14. SUBJECT TERMS	15. NUMBER OF PAGES
Electrocatalysis, methanol fuel cell, carbon monoxide, platinum, NMR.	30
	16. PRICE CODE

17. SECURITY CLASSIFICATION OR REPORT	18. SECURITY CLASSIFICATION ON THIS PAGE	19. SECURITY CLASSIFICATION OF ABSTRACT	20. LIMITATION OF ABSTRACT
UNCLASSIFIED	UNCLASSIFIED	UNCLASSIFIED	UU

Final Progress Report

New Electrocatalysts for Direct Oxidation of Organic Fuels

Elton J. Cairns and Jeffrey A. Reimer
Lawrence Berkeley National Laboratory
Berkeley, CA 94720

Grant # 48713CH

7/12/2005 – 5/22/09

Submitted to the Army Research Office

Robert Mantz, Program Manager

Table of Contents

List of Appendices, Illustrations, and Tables

Statement of the Problem

Direct alcohol fuel cells are an attractive alternative for supplying the Army with portable power. These devices could be used as chargers for rechargeable batteries, as well as stand-alone power supplies. While these systems have been shown to be technically feasible, their performance is currently much lower than needed, and they are expensive, due to the cost associated with high loadings of precious metal electrocatalysts. To supply the Army with portable, reusable power sources in the field, we are working towards new and better electrocatalysts for alcohol-powered fuel cells.

There is a large amount of literature available on the use of Pt, Pt-Ru, and other alloys of Pt with platinoid elements and transition metals for the electrocatalytic oxidation of methanol. [1-4] To date, the best combination of activity and stability has been obtained by the use of Pt-Ru, but high loadings are required for reasonable performance (100-200 mW/cm^2 at efficiencies of less than 25%). It has been difficult to develop improved electrocatalysts because of a lack of fundamental understanding of the relationships among composition, structure and electrochemical activity. The uniqueness of Pt as an electrocatalyst is not understood, so the atomic-level properties that provide electrocatalytic activity are not known. Some general guidance for electrocatalyst design is provided by the concept of the bimolecular reaction mechanism wherein a carbonaceous intermediate adsorbed on the electrocatalyst surface is more readily oxidized if the Pt site(s) on which the carbonaceous adsorbate resides are adjacent to sites that have an oxygen-containing adsorbate (such as OH or H_2O). [5-7] The nearby oxygenated species are available to participate in the oxidation reaction, and thus speed up the oxidation of the adsorbed carbonaceous intermediate. In the case of Pt-Ru, the Ru is known to adsorb oxygenated species at a low potential (lower than for Pt alone), enhancing the oxidation rate of methanol at these low potentials.

Consistent with the concept of the bimolecular reaction mechanism, we have been working on the development of new electrocatalysts that provide the oxygenated adsorbates at low potentials. In order to avoid the limitations of the available preparation methods, we have developed a new method for the preparation of high specific area alloy electrocatalysts, and have demonstrated its utility in the preparation of Pt-Ce and Pt-Pr alloys (which are very stable intermetallic compounds). [8-10] This technique opens up a large, previously unexplored composition space for the development of new electrocatalysts.

It has long been recognized that alloying platinum with other noble metals (such as ruthenium or palladium) can lead to an improvement in that material's ability to oxidize carbonaceous species from its surface. Further discovery of appropriate fuel cell electrocatalysts has been largely accomplished by alloying constituent metals into combinations with varying ratios, and then testing each new material for electro-oxidative activity. While varying degrees of success have been met with this approach, a commercially viable anode electrocatalyst for direct-alcohol fuel cells (meaning a more robust, active, and cheaper material) still has not been found.

The goal of this project is to understand at the atomic level the important features of active electrocatalysts, and to use this information for the design and synthesis of much more active electrocatalysts for the oxidation of liquid fuels acceptable to the US

Army for use in the field. Our approach is to understand the fundamental aspects of the surface chemistry in relevant electrochemical systems and use this information to uniquely tailor the catalytic surface for the Army's needs.

Background

There is a large amount of information that has been gleaned about platinum and platinum alloys from single crystal and spectroscopic studies [11-18] under both UHV and electrochemical conditions. It is widely believed that in an electrochemical environment, methanol adsorbs to a Pt surface as a species closely related to CO. We have drawn from this body of literature when analyzing our current results on methanol electro-oxidation from commercially available platinum alloys and novel materials developed in our labs. We find that methanol electro-oxidation is not as simple as the case for CO.

In this study, we find there are some important implications about the electro-oxidative activity of alloys that can be derived by simply studying the oxidation of CO (from gas) on platinum, particularly on unsupported platinum nanoparticles. The voltammetric behavior of CO on platinum can be used to understand what parameters are most important when tailoring the catalytic surface. This is especially useful when considering alloys for alcohol electro-oxidation, as alloys, unlike pure Pt, do not exhibit a well defined hydrogen region in the voltammogram that can give some indication of both the available number of active sites for catalysis and the type of site available. We must utilize spectroscopic characterization in addition to voltammetric studies to extract information about these systems.

Nuclear magnetic resonance spectroscopy (NMR) is particularly well suited to this study because of its ability to probe both sides of the electrocatalytic interface. In our labs, we have developed a unique electrochemical method and apparatus that allow us to tune the electrocatalyst's surface environment using voltammetry and adsorb methanol for the study of how potential and adsorbate characteristics affect the electronic structure of platinum (via ^{195}Pt NMR). We are then able to take that same sample and study how the electronic structure of the adsorbate is changed as a result of the platinum's local density of states (LDOS) via ^{13}C NMR. By combining this two-sided view of the catalytic interface with voltammetric studies, we can extract a wealth of information about the interactions on the surface, as well as a sense of the importance of different parameters in the design of the catalysts.

^{195}Pt NMR spectra of electrocatalyst nanoparticles (less than 100nm) are very broad. [19-21] For solid-state NMR studies of electrocatalytic systems, this breadth affords excellent resolution between the peaks for surface and bulk Pt atoms. The local magnetic field experienced by a nucleus is coupled to the total electron polarization, and the shift in resonant frequency, called a Knight shift, reflects this strong interaction. Where chemical shifts are usually on the order of tens of Hertz or less, Knight shifts can be on the order of 10^6 Hertz.

In general, the conduction electrons that interact most strongly with the nucleus occupy *s*- like orbitals (wave function overlap is maximized). Electrons exhibiting *d*- orbital character interact with the nucleus through a phenomenon known as core

polarization. [22, 23] The polarization of *d*- electrons polarizes the *s*- electron core, which then transfers polarization to the nucleus. It is generally recognized that *s*- character electrons impart a positive Knight shift and *d*- character electrons impart a negative Knight shift. Bulk Pt metal has predominantly *d*- character conduction electrons, resulting in a large negative Knight shift. The breadth of the Pt NMR spectrum for particles under 100nm arises from the non-uniformity in the electronic local density of states (eLDOS) in small particles. Platinum nanoparticles exhibit properties that deviate from those of bulk metallic Pt and microscopic variations in the Knight shift arise from the continuum of electronic environments ranging from bulk-like to surface-like as one moves from the inside to the outside of the catalyst particle. When coated with adsorbates, the intensity, size, and shape of the surface-sensitive side of the Pt spectrum vary with the type of adsorbate and with Pt particle size. It is this surface resolution that makes this technique useful in probing the surfaces of these electrocatalyst particles.

^{13}C-NMR is particularly well suited to study ^{13}CO (and $^{13}CH_3OH$) adsorbed to Pt, as the ^{13}C-NMR spectrum provides information on the structure, mobility, and electronic environment of the adsorbate. The ^{13}C-NMR spectrum of $^{13}CO_{ads}$ on Pt (or Pt-alloy) particles gives direct insight into the electronic structure at the surface of the catalyst, as the ^{13}C-NMR shift is dominated by metallic behavior, indicating significant mixing of the CO molecular orbitals with the Pt conduction electron bands. A greater electronic density of states at the Pt surface results in a greater NMR shift in the ^{13}C-NMR spectrum. [24,25] The width of the ^{13}C-NMR line for $^{13}CO_{ads}$ is also very informative: a narrow line is indicative of high surface mobility for the adsorbate. [26,27] Measurements of NMR relaxation timescales (including linewidth measurements) can be used to calculate the timescale of surface diffusion for CO_{ads} on Pt. In recent years, a molecular-level understanding has emerged on the nature of ^{13}C shifts observed for adsorbates, and for ^{195}Pt shifts observed in Pt particles. These studies provide the fundamental background necessary in order to interpret carbon and Pt shifts in other metal particle alloys. We have shown the applicability of ^{13}CO NMR towards the study of CO on practical fuel cell electrodes, and have reported NMR, coulometry and voltammetry studies of CO adsorbed onto carbon-supported platinum (Pt/C) electrocatalysts, leading to the formulation of an overall model for the adsorption and oxidation of CO on Pt in an acid electrolyte at ambient temperature. [28,29]

While ^{13}C-NMR provides information on the nature of the adsorbate and the electronic environment at the active surface of the fuel cell electrode, we get complementary information from cyclic voltammetry (CV) on the structure of the adsorbate, the number of electrons required for oxidation, and the overall electrochemical activity of the catalyst of interest (which is used as the *working electrode*). In CV, the potential of the working electrode is swept upwards and downwards relative to the potential of a reference electrode. As the potential is swept, surface reactions occur on the working electrode, resulting in an electrical current as electrons are released (oxidation, positive current by convention) or consumed (reduction, negative current). Examples of voltammograms and their interpretations are discussed below.

By combining our spectroscopic data with voltammetric results, we are able to draw conclusions about electronic structure and mechanistic roles in producing an ideal catalytic surface for a reaction of interest. We will use this information to further develop the spectroscopic tools necessary to appropriately study methanol oxidation on alloy

surfaces, which cannot be studied as completely as Pt using electro-analytical methods because of the smaller, featureless hydrogen region of the voltammogram.

Summary of Results

CO and CH_3OH on Pt/C

During the first year of the project we carried out an examination of carbon-supported platinum electrocatalysts [30]. Combined electrochemical and ^{13}C NMR studies of adsorbed methanol on Pt/C electrocatalysts have shown very interesting differences between adsorbed CO and adsorbed CH_3OH. Methanol is adsorbed preferentially onto Pt(100)-like sites (associated with strongly-bound hydrogen (SB sites)) because it requires dehydrogenation on adsorption, and Pt(100) is a better dehydrogenation catalyst than Pt(110) or Pt(111). Because CO does not require dehydrogenation as it adsorbs, it adsorbs rapidly onto both Pt(110) (weakly bound H sites (WB sites) and Pt(100) (SB sites). For the oxidation process, the adsorbates from CO and from CH_3OH behave very similarly, rapidly oxidizing from the Pt WB sites, and more slowly from the Pt SB sites. These results are summarized in Table 1. [31]

Table 1. Relative adsorption and oxidation rates of CH_3OH on Pt SB and Pt WB Sites for Pt/C Electrocatalysts

	Pt(SB)	Pt(WB)
CH_3OH adsorption	**fast**	**slow**
CH_3OH_{ads} oxidation	**slow**	**fast**
CO adsorption	**fast**	**fast**
CO_{ads} oxidation	**slow**	**fast**

By combining results from electrochemical and NMR studies of the adsorbates resulting from CO and methanol adsorption, we have found that there is a strong connection between the NMR shift of the ^{13}C NMR peak and the type of surface site occupied by the adsorbate. This is the case because the ^{13}C NMR peak is Knight-shifted, reflecting an interaction between the ^{13}C nucleus and the conduction electrons in the Pt. The shift for the CO on the Pt WB sites is larger than that for the CO on the Pt SB sites because of the higher electronic density of states for the more closely-packed Pt atoms on the 110-like WB sites than for the 100-like SB sites. This provides us with a useful tool for assessing the relative coverages on different surface sites.

We have successfully synthesized $PrPt_2$ and $CePt_2$ via a novel synthetic technique developed in our labs.[32] These materials are high surface area electrocatalyst powders, as seen by BET and TEM studies. The crystal structures of the two alloys are similar to each other as seen by XRD and XAS. This is expected from the close proximity of cerium and praseodymium on the periodic table. From NMR studies, we observe that the electronic structure of both these materials results in the opposite Knight shift observed in

platinum black and other platinum-based electro-oxidation catalysts.[30] NMR is capable of probing the small changes in LDOS and as a result, provides good surface sensitivity. In addition to the interesting electrocatalytic properties observed previously in these new materials, they should provide valuable information regarding correlations between electronic structure and electrocatalytic activity.

CO and CH_3OH on Pt Black

In the second year, we extended our study to unsupported electrocatalysts that are of greater interest for direct methanol and direct ethanol fuel cells. We have developed a new *in situ* NMR electrochemical cell for this work, as described below.

The use of platinum as a reference electrocatalyst has been very helpful, as it has allowed a detailed study of the coverages of bridged and linear CO adsorbate, and the behavior of these adsorbates on the close-packed (weakly-bound H) sites and the cubic (strongly-bound H) sites. The new NMR electrochemical cell shown in Figure 1 proved to be very useful in obtaining both electrochemical and NMR data for samples of CO_{ads} surfaces prepared under a variety of conditions, allowing full characterization of the adsorption and oxidation properties of adsorbates prepared from CO gas and CH_3OH.

This study has revealed the influences of adsorbate structure (bridged vs. linear), coverage, and type of surface site on the relative adsorption rate and electrooxidative activity of the electrocatalyst. Figure 2 shows sample voltammograms for the behavior of CO gas adsorbed onto a Pt black electrode. Note the dual-peak structure of the oxidation current for the adsorbed CO. The inset in Figure 2 shows the voltammetry of the hydrogen region, which indicates the preferential oxidation of CO_{ads} from the weakly-bound (WB) hydrogen sites. The dual peak behavior of the CO oxidation is associated with the different kinetics experienced on the WB and SB sites of the Pt. The kinetics of this situation was analyzed using a modified Butler-Volmer expression for each of the two types of surface site:

$$i = A\left(xk'_1 Exp\left[-\frac{k'_1}{2\nu\alpha_1 f} Exp[2\alpha_1 fE] + 2\alpha_1 fE \right] + (1-x)k'_2 Exp\left[-\frac{k'_2}{2\nu\alpha_2 f} Exp[2\alpha_2 fE] + 2\alpha_2 fE \right] \right) \quad (1)$$

Where:

$$\nu = \frac{dE}{dt}$$

$$E_{rev} = 0$$

$$A = 2FN_{CO,t=0}$$

$$k' = k\theta_{OH}$$

$$f = \frac{F}{RT}$$

This kinetic expression fits very well the experimental data, as indicated by the sample fit shown in Figure 3. A more complete description of the model and the experiments is provided in [33]. We have found that the highest activity for the oxidation of the methanol adsorbate is for bridge-bonded CO on close-packed (weakly-bound H) sites, and at intermediate coverages, allowing for adequate OH_{ads} [33]. The overall rate behavior of CO and CH_3OH at low potentials for unsupported Pt black is the same as shown in Table 1 [34]. The results for the analysis of the voltammetry for the CO_{ads} from CO gas and CH_3OH are summarized in Figure 4 [33]. Note the consistency of the results for CO gas and CH_3OH.

Interpretation of NMR Peak Shifts

The electrochemical results discussed above are very useful in the interpretation of the trends in the ^{13}C NMR shifts with surface coverage by CO_{ads}. We have found a consistent trend of NMR peak shifts with the relative surface coverage of CO_{ads} on the WB and SB Pt surface sites [35]. Figure 5 shows the shifts in the ^{13}C NMR peaks observed with changes in surface coverage of the methanol adsorbate during adsorption and oxidation. Taking into account the results from the voltammetric studies, it is expected that the ^{13}C NMR peak experiences a larger Knight shift for the $^{13}CO_{ads}$ on the more densely-packed WB sites, and a smaller Knight shift for the $^{13}CO_{ads}$ on the SB sites. As discussed in [C], there is the expected relationship between the NMR shift and the relative amounts of CO_{ads} on the WB and SB sites. This relationship is shown in Figure 6. For each type of electrocatalyst, the data fall on a clear trendline. The reason for the two different lines is attributed to a support effect, influencing the electronic density of states for the two electrocatalysts. For a more complete discussion, see [35].

These results should be very useful in the study of Pt alloy electrocatalysts since the alloys do not offer a well-defined hydrogen region in the CV's. This makes it infeasible to assess the surface coverages on the different families of surface sites using CV. With the aid of NMR, we expect to be able to use the NMR peak shifts as indicative of relative coverages on the different types of surface sites.

CO_{ads} Mobility on Pt

Since we have observed that methanol is most rapidly adsorbed onto the Pt SB sites, but most rapidly oxidized (at low potentials) from the Pt WB sites, it is important to understand the mobility of CO_{ads} on the surface of the Pt electrocatalyst. To this end, we have used ^{13}C NMR to study the mobility of the CO_{ads} on the electrocatalyst surface.

Because of the breadth of the 13C NMR line, and because we observe long lifetimes for the ratio of WB:SB site occupation, we propose a model of two-site

chemical exchange between our WB and SB sites, with rapid diffusion within the WB and SB sites, as the mechanism of motion on our saturated COads on platinum black surfaces. This type of concerted motion would prevent an equalization of site population, and would account for the lack of redistribution between WB and SB sites that we observe. Faster diffusion within a family of sites between linear- and bridged- bound species averages the interaction between different binding modes and the metal surface.

In order to test this model, we probe the effect of 180-pulse spacing on the measured experimental T2 from a CPMG sequence's echo amplitude decay. CPMG sequences are composed of a 90-pulse, followed by a delay time τ_d, followed by a series of 180-pulses with each separated by a time $2 * \tau_d$. In principle, T2 can be measured by monitoring the echo amplitude as a function of time. This is illustrated in Figure 7.

The effects of chemical exchange on the decay of echo amplitudes in CPMG echo trains has been well established [36-41]. In particular, it has been applied to the case of chemical exchange in biomolecular systems and for probing the dynamics therein [41-44]. The time, t_{cp}, is the time between 180-pulses, defined as

$$t_{cp} = 2 * \tau_d + \tau_{180-pulse} \qquad (2)$$

For long delay times in the presence of diffusion, species under observation have some probability of jumping to different sites within the sample. This will lead to a faster decay in signal than would be the case without the presence of motion.

The catalysts used in this study are unsupported, fuel cell grade platinum black catalysts (Sigma-Aldrich). The sample studied here is made of an electrode stack to allow for both spectroscopic and electrochemical probing of the platinum surface [29, 31,45]. Catalyst inks were prepared using a mixture of Nafion-117 solution (Scientific Polymer Products, Inc., hydrogen ion form, 5% solids, 10% water, balance lower aliphatic alcohols) and platinum black. For this work, these inks were applied and dried onto one side of cut glass slides coated with a 1μm layer of gold. The catalyst loading of each electrode is approximately 4 mg/cm2 . Each electrode is connected by a gold wire (0.005 in., Englelhard Corporation) and multiple electrodes are arranged to form a cylindrical electrode stack sample, which acts as a working electrode. This stack is housed in a custom built flow cell that allows for methanol to be electrochemically adsorbed to the platinum surface and for flushing the stack to remove any dissolved methanol [Figure 1].

Cleaning of the platinum surface was performed by potential cycling using a PAR

263A potentiostat. Our flow cell uses a platinum mesh counter electrode, and a Hg/HgSO4 reference electrode (Koslow Scientific). The clean platinum surface was recorded using CV. Methanol was adsorbed onto the stack from a 1.5M $^{13}CH_3OH$ (^{13}C, 99%, Cambridge Isotopes) / 0.5M H2SO4 (Certified ACS Plus Grade, Fisher Scientific) solution DI-water filtered in a Millipore Organ-X system (18M). Adsorption was performed at 250 mV vs RHE for 3h and full coverage was monitored by sweeping the low potential hydrogen region. After full coverage was achieved, the cell was rinsed with DI-water and the valves were closed for removal of the contained sample to the NMR set-up.

In this work, we measure the effect of varying t_{cp} on the measured T_2 . ^{13}C NMR experiments were performed on a Tecmag Lab NMR spectrometer at a field of 7.04T using a 1μs dwell time. The electrode stack design [29,31,45-47] is depicted in Figure 1

and enables approximately $3m^2$ of surface area to be contained in a sample approximately 1 cm in diameter. The use of a gold film as the current collector to support our electrode helps minimize carbon background signals, though some do exist from sources outside the coil. Large pulse powers (~1kW) are required to uniformly excite the electrode stack. Using a homebuilt probe that can accommodate our large sample size, we can achieve a 4.5μs 90-pulse, and a 10μs 180-pulse. The 180-pulse is not exactly twice our 90-pulse because of our large sample coil. The t_{cp} times range from 25μs to 160μs.

Two surface coverages were used at 293K, a saturated layer and a CO_{ads} coverage resulting after 5min. of partial oxidation at 450mV vs. RHE. CPMG data were also acquired from the saturated layer at 283K. Additional experimental details are provided in [48].

The model for two-site exchange relates the relaxation time constant to the t_{cp} time as follows:

$$R_2 = \frac{1}{T_2} = \frac{R_{2A} + R_{2B} + p_B k_{ex} + p_A k_{ex}}{2} - \frac{1}{t_{cp}} ln\lambda^+ \qquad (3)$$

Where:

$$\begin{aligned}
ln[\lambda^+] &= ln[(D_+ cosh^2\xi - D_- cos^2\eta)^{1/2} + (D_+ sinh^2\xi - D_- sin^2\eta)^{1/2}] \\
\zeta &= 2\Delta\omega(R_{2A} - R_{2B} + p_B k_{ex} - p_A k_{ex}) \\
\psi &= (R_{2A} - R_{2B} + p_B k_{ex} - p_A k_{ex})^2 - \Delta\omega^2 + 4 p_A p_B k_{ex}^2 \\
\eta &= \frac{1}{\tau_{cp}\sqrt{8}} \sqrt{-\psi + \sqrt{\psi^2 + \zeta^2}} \\
\xi &= \frac{1}{\tau_{cp}\sqrt{8}} \sqrt{+\psi + \sqrt{\psi^2 + \zeta^2}} \\
D_+ &= \frac{1}{2}(+1 + \frac{\psi + 2\Delta\omega^2}{\sqrt{\psi^2 + \zeta^2}}) \\
D_- &= \frac{1}{2}(-1 + \frac{\psi + 2\Delta\omega^2}{\sqrt{\psi^2 + \zeta^2}}).
\end{aligned}$$

The values of p_A and p_B, the surface populations of $^{13}CO_{ads}$ on the WB and SB sites, are obtained from the voltammetric experiments, and the values of T_{2A}^o and T_{2B}^o are obtained from the literature (1.4 ms). This leaves Δω, the frequency difference for the NMR lines for the CO_{ads} on the two types of surface sites, and k_{ex}, the exchange rate for CO_{ads} between the two types of sites, to be obtained from the NMR results here. The

results in Figure 8 are fitted to the above equation by adjusting the values of $\Delta\omega$ and k_{ex}. The best fit is obtained for $\Delta\omega$ = 19.9 kHz, and k_{ex} = 48080 $s^{-1.}$

Further analysis as to the validity of the two-site exchange model probed with CPMG is attempted by fitting the ^{13}C NMR lineshape directly. As mentioned earlier, our model involves two types of motion, fast diffusion within a family of sites, and a slower chemical exchange between the two types of sites. The ^{13}C lineshape is modeled as two individual sites, with exchange between the two sites. As is well known [49], there are two predominant regimes of motion for this case. In the slow intermediate exchange regime, motion between the two sites causes a blurring of the two distinct lines associated with the respective sites. As the timescale of the exchange approaches the average for the difference in resonant frequency of the two sites, the lines broaden, coalesce, and eventually appear to be a single broad line. As the motion between the two types of sites increases even further, the broad single line begins to narrow. The motion becomes so fast that on the NMR timescale, one can no longer distinguish between two different sites. The molecules themselves begin to experience a field that is essentially the average of those for the two types of sites. Very fast averaging in this regime will eventually result in a single narrow line. This is called the fast exchange regime. We consider slow intermediate exchange as the regime for exchange between sites on our catalysts because of the breadth and asymmetry of the 13C NMR line.

Motion in the fast exchange regime would result in an apparent single peak resulting from the averaging of shifts from the two different sites. Though an increase in temperature does result in a narrowing of the ^{13}C NMR line [50], the asymmetry indicates that this rate must be on the order of or less than the frequency difference between the two sites. The narrowing of the 13C NMR line is attributed to fast diffusion within a family of sites, similar to the hypothesis of fast diffusion on faces made by [51]. The equation used to fit our ^{13}C NMR lineshape in the slow intermediate two-site exchange regime is:

$$M = -C_0 \frac{P\left[1+\tau\left(\frac{p_B}{T_{2A}}+\frac{p_A}{T_{2B}}\right)\right]+QR}{P^2+R^2} \tag{4}$$

$$P = \tau\left[\frac{1}{T_{2A}T_{2B}} - 4\pi^2\Delta\nu^2 + \pi^2\delta\nu^2\right] + \frac{p_A}{T_{2A}} + \frac{p_B}{T_{2B}}$$

$$Q = \tau[2\pi\Delta\nu - \pi\delta\nu(p_A - p_B)]$$

$$R = 2\pi\Delta\nu\left[1+\tau\left(\frac{1}{T_{2A}}+\frac{1}{T_{2B}}\right)\right] + \pi\delta\nu\tau\left(\frac{1}{T_{2B}}-\frac{1}{T_{2A}}\right) + \pi\delta\nu(p_A - p_B)$$

$$\delta\nu = \nu_A - \nu_B, \Delta\nu = 0.5(\nu_A + \nu_B) - \nu, \tau = \frac{1}{k_{ex}}$$

Where: M is the intensity of the NMR signal

C_o normalizes the result to the ^{13}C population on the surface
ν_A and ν_B are the frequencies for the MNR lines for CO_{ads} on the two types of surface sites
k_{ex} is the exchange rate (s^{-1})

This equation accounts for the unequal populations between the two sites. In this equation, p_A refers to the population of the higher frequency (WB) sites and p_B refers to the population of the lower frequency (SB) sites. (It should be noted, that the form of this equation defines site A and B with the opposite convention as the equation used for CPMG analysis.) Frequency units are used directly in these equations and the exchange rate is in s^{-1}. Using the parameters derived from the fit to our CPMG data, we are unable to fit the 13C NMR lineshape well. This is illustrated in Figure 9, which takes the parameters from the best fit of the CPMG data, and plots the corresponding lineshape. The values from the CPMG fit give a calculated broader linewidth than the actual data and the calculated rate of exchange is not high enough to result in the collapse of the two separate peaks into one, like the single asymmetric peak observed in the literature.

To explore this in more detail, the ^{13}C NMR lineshape is instead fitted independently, assuming the same population coverages and an R_2 of 700/s (T_2 = 1.4ms). This R_2 is chosen because it is a reasonable value, based on literature values for T_2 from gas phase adsorption work. It is also used as our rough estimate because it correlates with the best fit from the CPMG experiments. From this assumption, the ^{13}C NMR line is fit and values for k_{ex} and the shifts for each site are calculated. The fit to our lineshape seen in Figure 10 is very reasonable, with a frequency difference of about 13kHz and a k_{ex} = 62671/s. Importantly, it captures the asymmetry and breadth of the ^{13}C NMR line, which has often been observed in our group and others, but not sufficiently explained [28, 29,35, 51-53]. Additionally, a difference of 13kHz is close what we expect from analyzing the frequency shift dependence on coverage of WB and SB sites in [35]. This lineshape fit is not extremely sensitive to the T_2 used for the individual sites. A choice of a shorter T_2 , like R_2 = 1400, gives a fit where the frequency difference is 12.4 kHz and k_{ex} = 60072/s.

For a line as broad as those for CO_{ads} on Pt, the dominating factors are the frequency difference between the two sites and the exchange rate between those sites. The parameters from the fit where R_2 = 700 are substituted into the CPMG model, and a theoretical R2 dependence on 1/tcp is calculated. This line is plotted and compared to our experimentally measured data in Figure 11. With the assumed T_2 of 1.4ms, the R_2 model line is a reasonable shape compared with our data. The calculated kink is in the same range of 1/tcps and the R_2s at high and low values of 1/tcp span a similar range. The obvious difference between measured R_2s and the model based on parameters from the lineshape analysis is an offset in inverse relaxation rates (an apparent translation to lower R_2 values calculated from the lineshape parameters). Because the shape of the generated CPMG analysis in Figure 11 follows that of our experimental data, this raises the possibility that perhaps there is some other relaxation mechanism in our system that is not accounted for in the R_2 vs. 1/tcp equations, but is forcing a faster experimentally observed relaxation time. This could explain why our exchange rates from the two models (CPMG and lineshape analysis) do not agree. One possible additional relaxation

mechanism could be the interaction between the labeled CO_{ads} on our platinum surface and protons in the water surrounding our catalyst.

At 80K, CO on platinum surfaces has additional relaxation mechanisms associated with surface C-C and C-Pt dipolar coupling, along with C-H coupling from water above the platinum surface. NMR studies of electrocatalytic surfaces at low temperature are done in deuterated water to remove T_2 decay associated with C-H coupling. We would expect that motion at high temperatures (such as 298K) would average away the effect of this in our system. The effect of C-H coupling on T_2 of the individual sites would probably have little effect on the ^{13}C NMR lineshape, as its breadth and shape are most strongly affected by the populations on the individual types of sites and k_{ex} and T_2. However, it is possible that C-H coupling could increase the effective relaxation rate of the system as a whole, resulting in smaller T_2 s (larger R_2s). Since Equation 2 does not account for this additional relaxation term, we would expect CH coupling to result in a shift of the R_2s dependence on $1/t_{cp}$ to larger R_2 values. To test this, we are in the process of evaluating C-H couplings by repeating the CPMG experiments in deuterated water.

The dependence of R_2 on 1/tcp in the case of a saturated surface supports our model of two-site exchange as a mechanism for diffusion of CO_{ads} on platinum electrocatalysts. A two-site model yields a calculated ^{13}C NMR lineshape that captures the breadth and asymmetry observed in the NMR line, an important feature that has not been previously explained. Though the two approaches we have explored do not yield exactly the same exchange rates and frequency differences between the two types of sites, it is possible that there are other relaxation mechanisms not accounted for in the CPMG model that can explain the discrepancy. The two-site view of the electrocatalytic surface is self consistent with many of the experimental results, including the observed NMR shift dependence on surface coverage, which we resolved by studying the behavior of the hydrogen region during adsorption and oxidation of surface species from CO(g) and CH_3OH . This two-site model is also supported by the observed appearance and deconvolution of the CO_{ads} oxidation peak during anodic voltammetric sweep experiments. Additionally, our model accounts for the bridged- and linear- species which are known to exist on the surface from other techniques. These results are somewhat surprising given the complex and disordered nature of a small metal particle surface. Even on small particles, however, clear differences in sites' activity can be seen by examining the hydrogen adsorption and desorption behavior. In light of this, our extension of this to the behavior of CO_{ads} on the different types of surface sites becomes less surprising.

The information gained from the Pt study is expected to be very useful in the analysis of the oxidation data for the Pt alloy electrocatalysts, beginning with Pt-Ru. The ^{13}C NMR methods we have developed will be very useful in interpreting data for the Pt alloy electrocatalysts, since it is not likely that voltammetry in the hydrogen region will provide detailed surface coverage information. Figure 12 illustrates this point. Only pure Pt shows clear peaks that are useful in assessing surface coverage and amount of electrochemically active surface. All of the Pt alloys show poorly-defined regions of hydrogen adsorption and oxidation. Other techniques must be used to assess surface area and surface coverages by adsorbates.

Initial data of several types have been gathered for some of the Pt alloys, and the examination of Pt alloy electrocatalysts will continue, using the results for Pt as a guide in our interpretations.

Summary

• CO(g) and CH_3OH adsorb onto and are oxidized from two types of Pt sites: weakly-bound (WB) hydrogen closely-packed (110-like) sites, and strongly-bound (SB) hydrogen loosely-packed (100-like) sites.

• Relative rates of adsorption have been measured for CO(g) and CH_3OH on the two types of Pt sites.

• The CV for CO_{ads} oxidation has been modeled and deconvoluted, and CO_{ads} oxidation rate constants have been measured for various surface coverages.

• The $^{13}CO_{ads}$ NMR results are consistent with the two-site model. The NMR peak shift quantitatively indicates the relative occupancy of the two types of sites.

• The $^{13}CO_{ads}$ NMR peak shape and relaxation times are consistent with a two-site exchange model for CO_{ads} mobility on Pt surfaces. The exchange rate constant has been measured, and the frequency difference for the ^{13}CO NMR lines corresponding to the two types of sites has been determined.

• Preliminary data have been gathered for some Pt alloys, including the Pt-Ln alloys synthesized in this project.

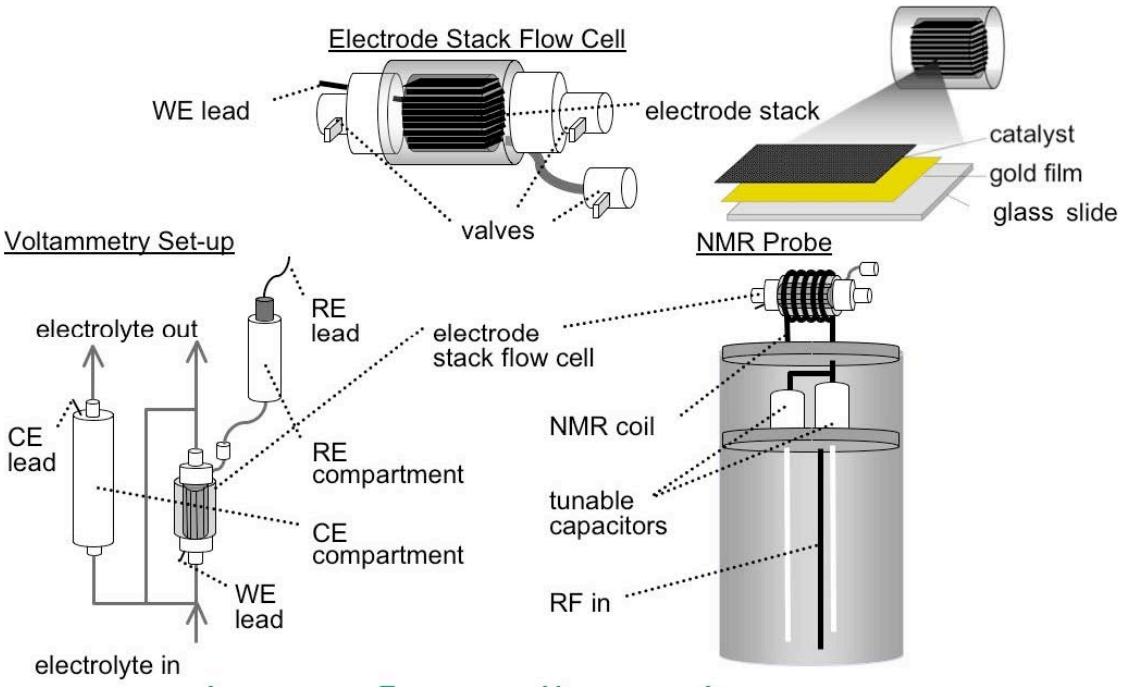

Figure 1. Schematic of Electrochemical / NMR setup. Insert in upper right depicts the electrode stack, made from an electrocatalyst ink dried into a thin gold film. CE, RE, and WE are counter, reference, and working electrodes, respectively.

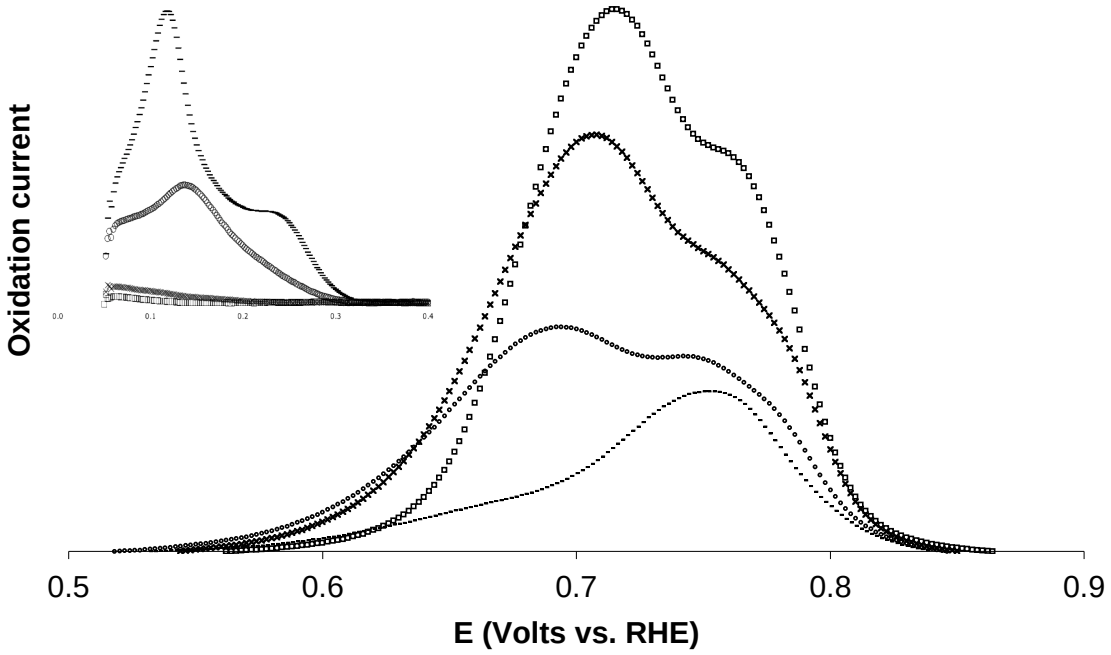

Figure 2. CO_{ads} (from CO) oxidation currents after partial oxidations at 450 mV: Squares: 5-minute partial oxidation, Exes: 20-minute, Circles: 60-minute, Dashes: 120-minute. Sweep speed: 25 mV/s. Inset shows corresponding hydrogen region.

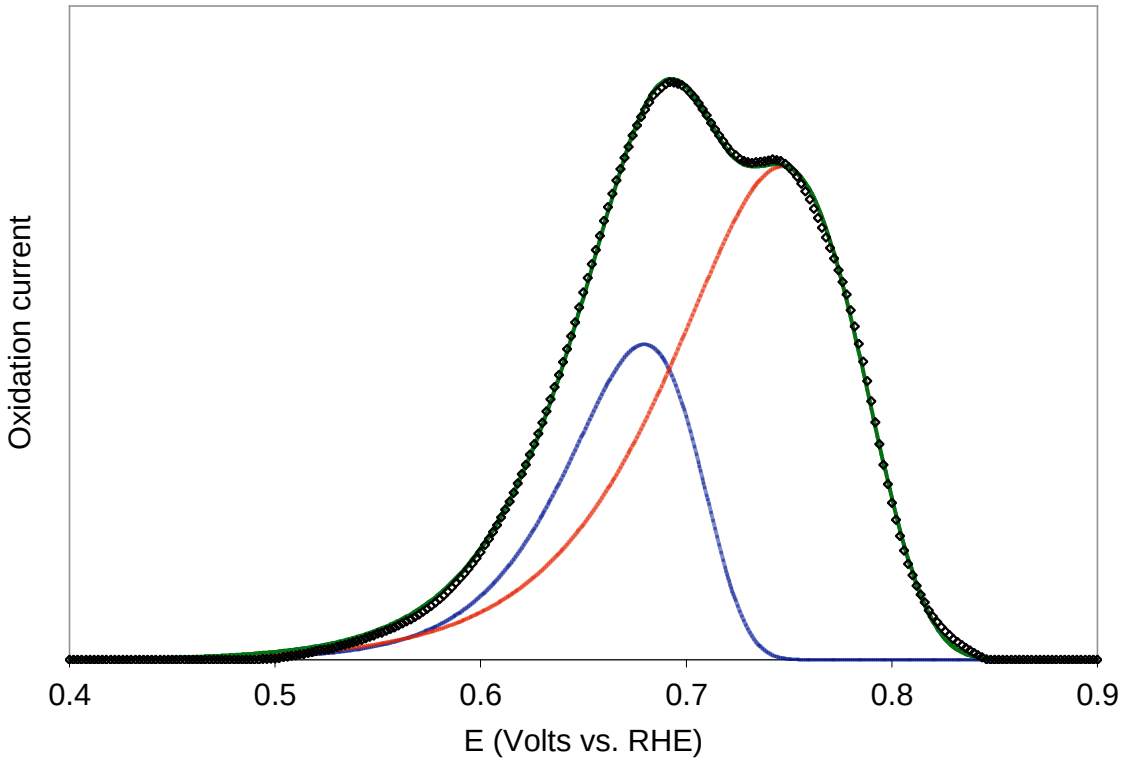

Figure 3. Oxidation current of CO_{ads} from 60-minute partial oxidation from CO gas adsorbed at 250mV (black diamonds) with total model fit (green curve). The two contributions to the total model fit are shown in red and blue. The parameters for this fit are A= 0.133 C, x= 0.31, α_1= 0.41,α_2= 0.29, $k_1' = 3.67*10^{-10}$ /s, and $k_2' = 2.81*10^{-8}$ /s.

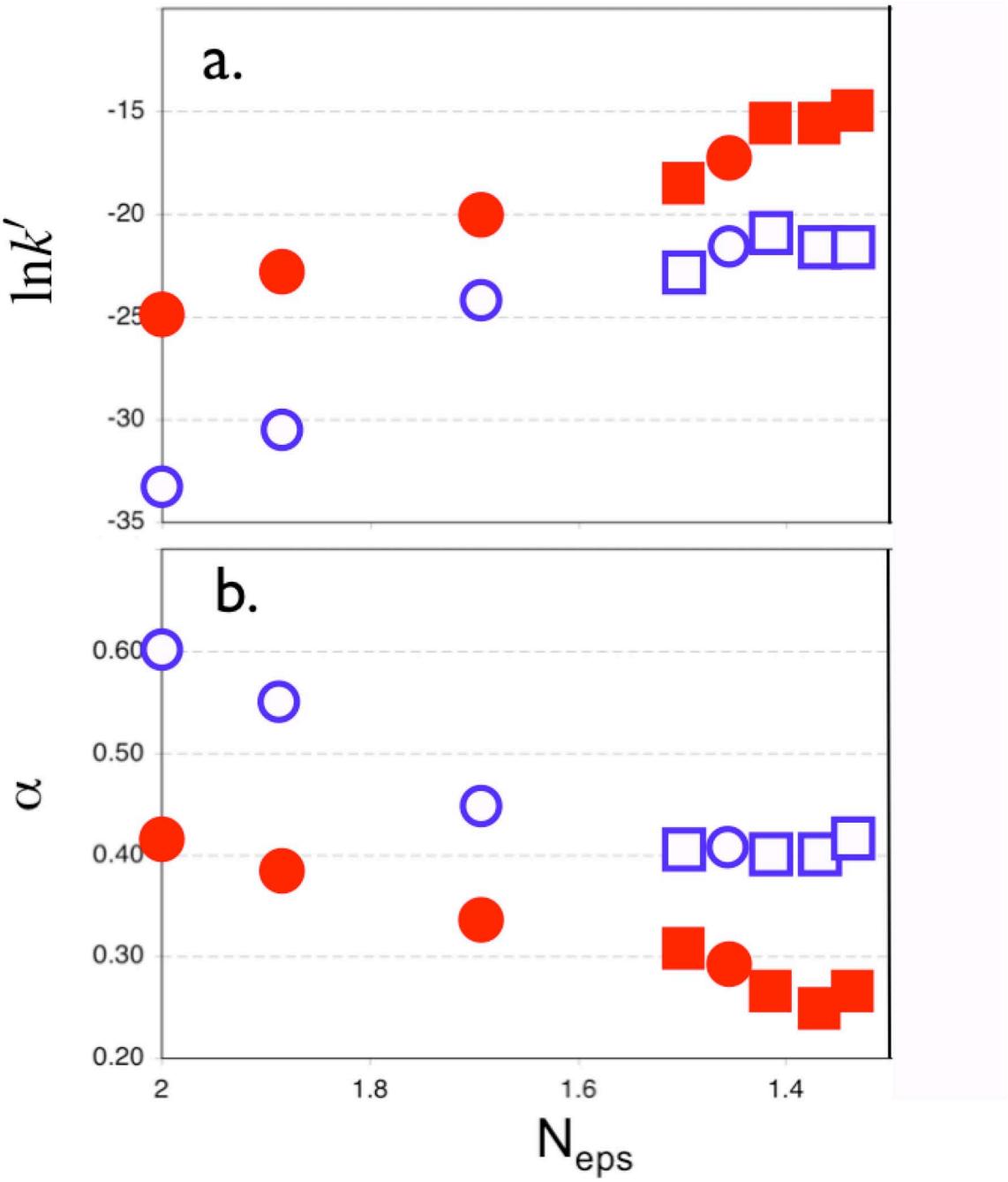

Figure 4: a) ln(k'$_i$) vs N_{eps} (number of electrons required for CO oxidation per Pt site vacated) for various preparations. O are for CO-derived adlayers and □ are for CH_3OH-derived adlayers. b) α_i vs N_{eps} for various preparations. O are for CO-derived adlayers and □ are for CH_3OH-derived adlayers. Hollow points correspond to Peak 1(~0.69V) and filled correspond to Peak 2(~0.75V) of the CO_{ads} oxidation peak envelope.

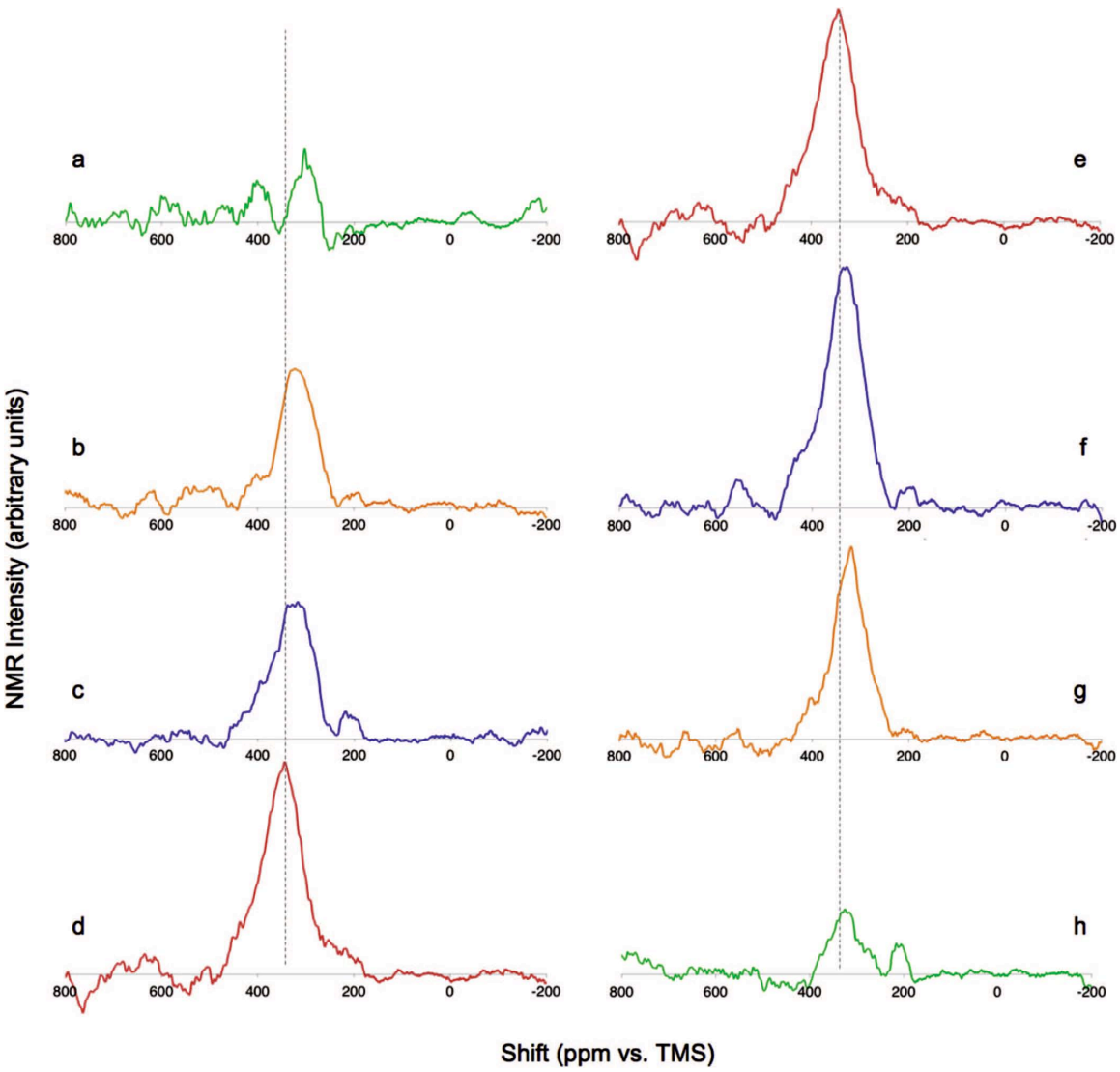

Figure 5. Representative 13C NMR spectra from electrode stacks after various surface preparations using $^{13}CH_3OH$. Plots to the left show spectra for a Pt/C electrode stack after partial adsorptions for (a) 10s, (b) 1 min, (c) 1 h, and (d) 12 h with 50 mM $^{13}CH_3OH$. Plots to the right show spectra for a Pt/C electrode stack after partial oxidations of the ^{13}CO-saturated surface, created through potential sweeps to (f) 550 mV, (g) 600 mV, and (h) 650 mV vs RHE. (e) ^{13}C spectrum of the saturated surface preparation before partial oxidation.

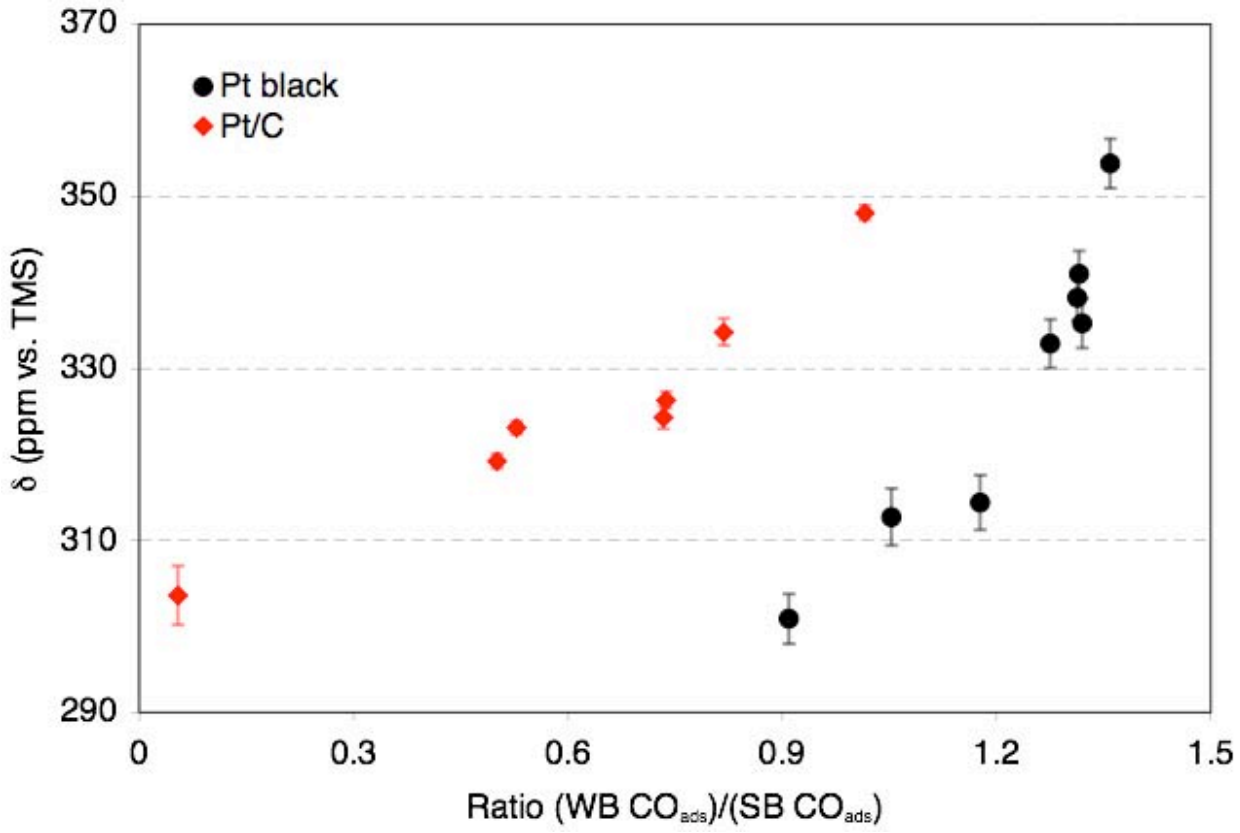

Figure 6. NMR shift (obtained from line shape fits) vs ratio of CO_{ads} occupation on WB and SB sites (obtained by cyclic voltammetry). Red diamonds represent data from Pt/C catalyst; black circles represent data from unsupported Pt black catalyst.

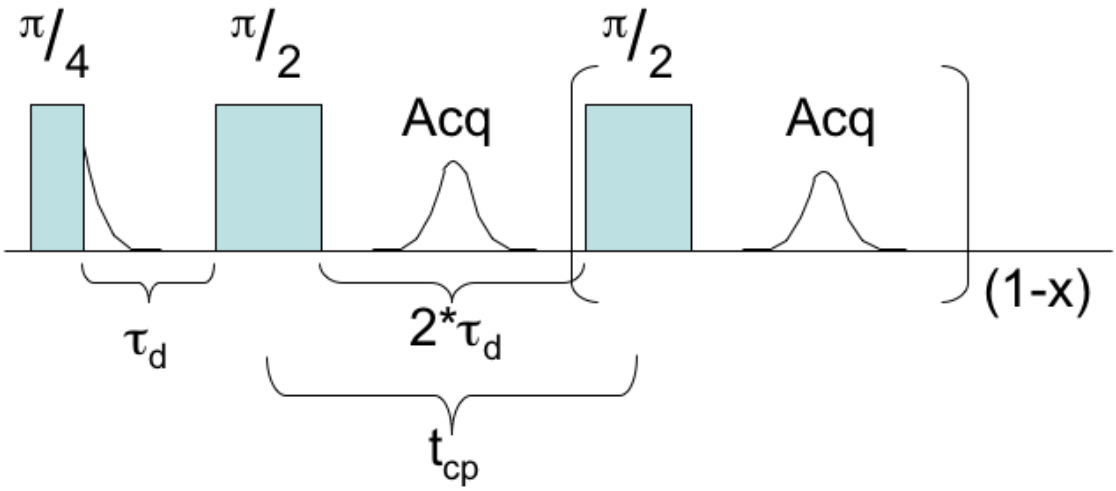

Figure 7: Cartoon of pulse sequence used for the CPMG experiments. The CP time, t_{cp}, is twice the echo delay, τ_d, plus the time for the 180-pulse. The 180-pulse is repeated x times, and the acquired echo is integrated to calculate T_2 .

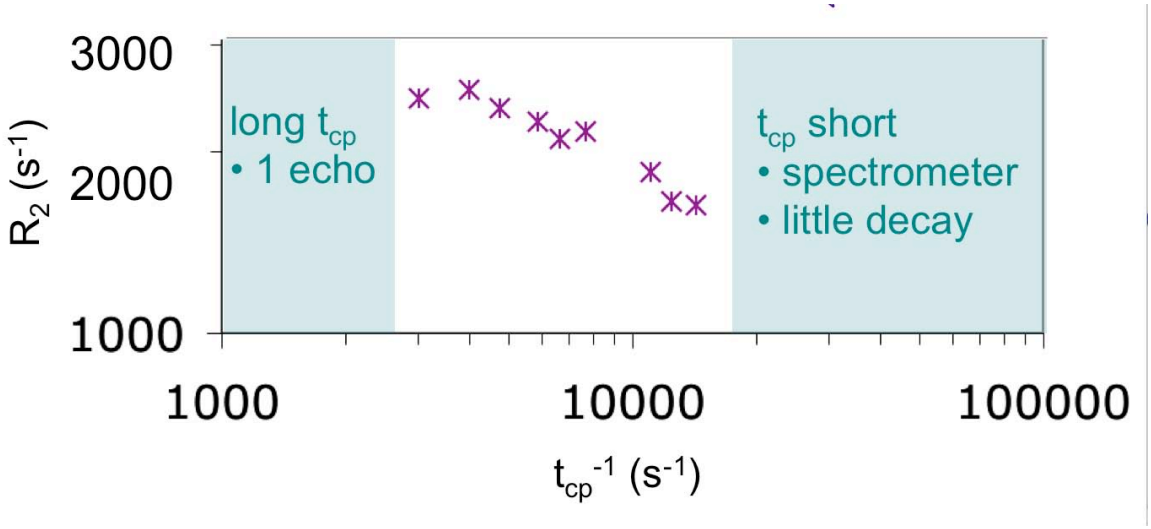

Figure 8: Log-Log plot of R_2 vs. $1/\tau_{cp}$ data for the saturated surface. R_2 is that experimentally determined from CPMG data fit to a single exponential

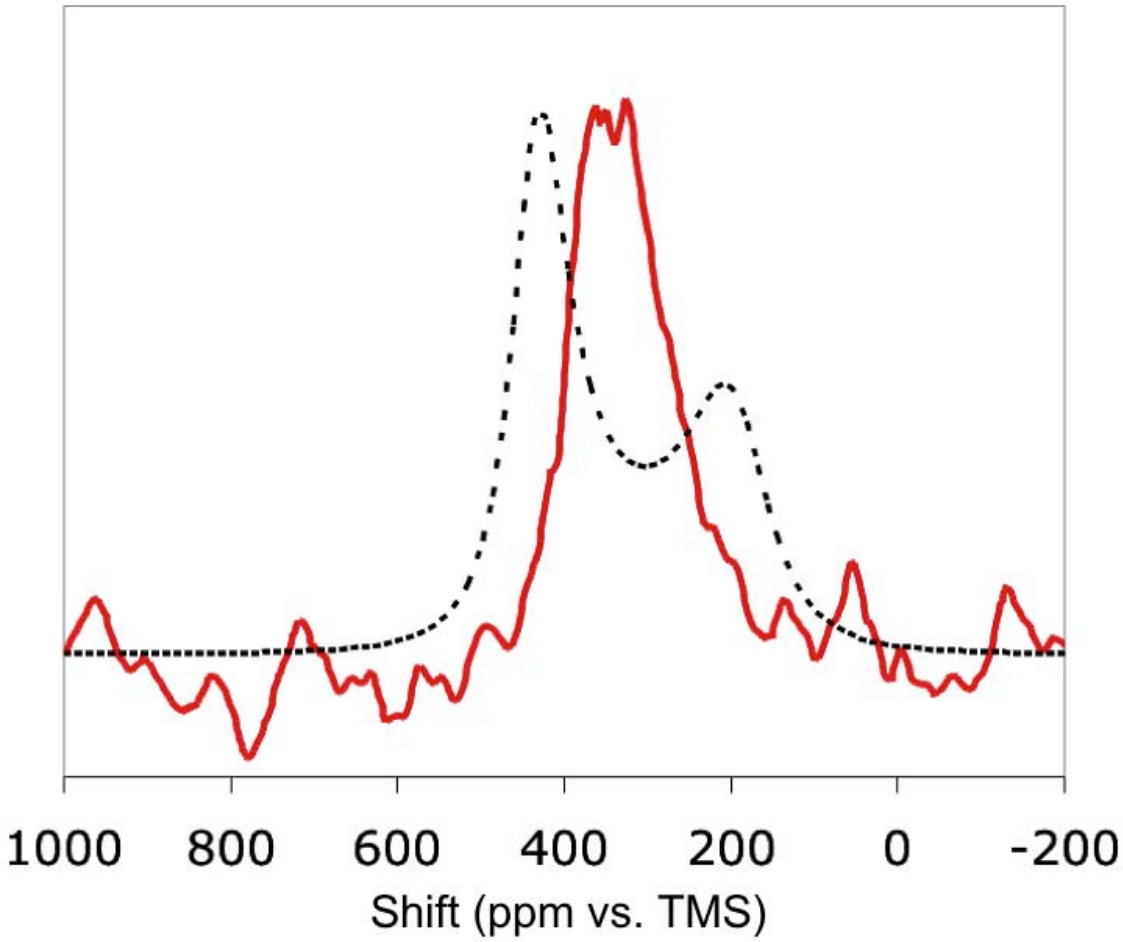

Figure 9: 13C NMR lineshape is plotted as a solid line in ppm (vs. TMS). A lineshape model for two-site exchange is also plotted using the best fit parameters from the CPMG data: T2 = 1.4ms for both sites, kex = 48080/s, _! = 19910/s, and the fractions for WB (0.58) and SB (0.42) sites used from voltammetry data.

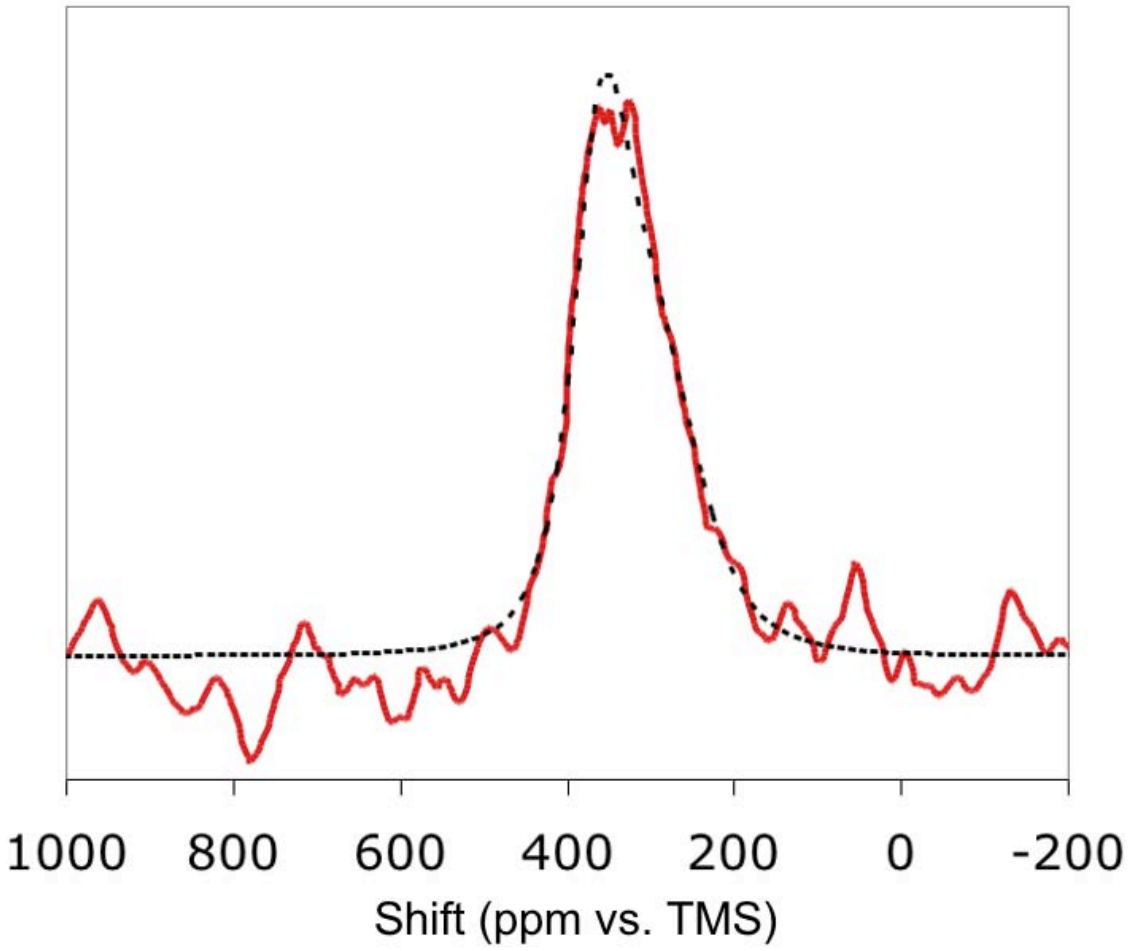

Figure 10: 13C NMR lineshape is plotted as a solid line in ppm (vs. TMS). The lineshape model for two-site exchange is fit to our data by assuming T2 = 1.4ms for both sites and by using the fractions of WB (0.59) and SB (0.41) sites calculated from voltammetry data. The resulting fit gives k_{ex} = 62671/s, and ν_A = 75.531MHz and ν_B = 75.518MHz, a difference of about 13kHz.

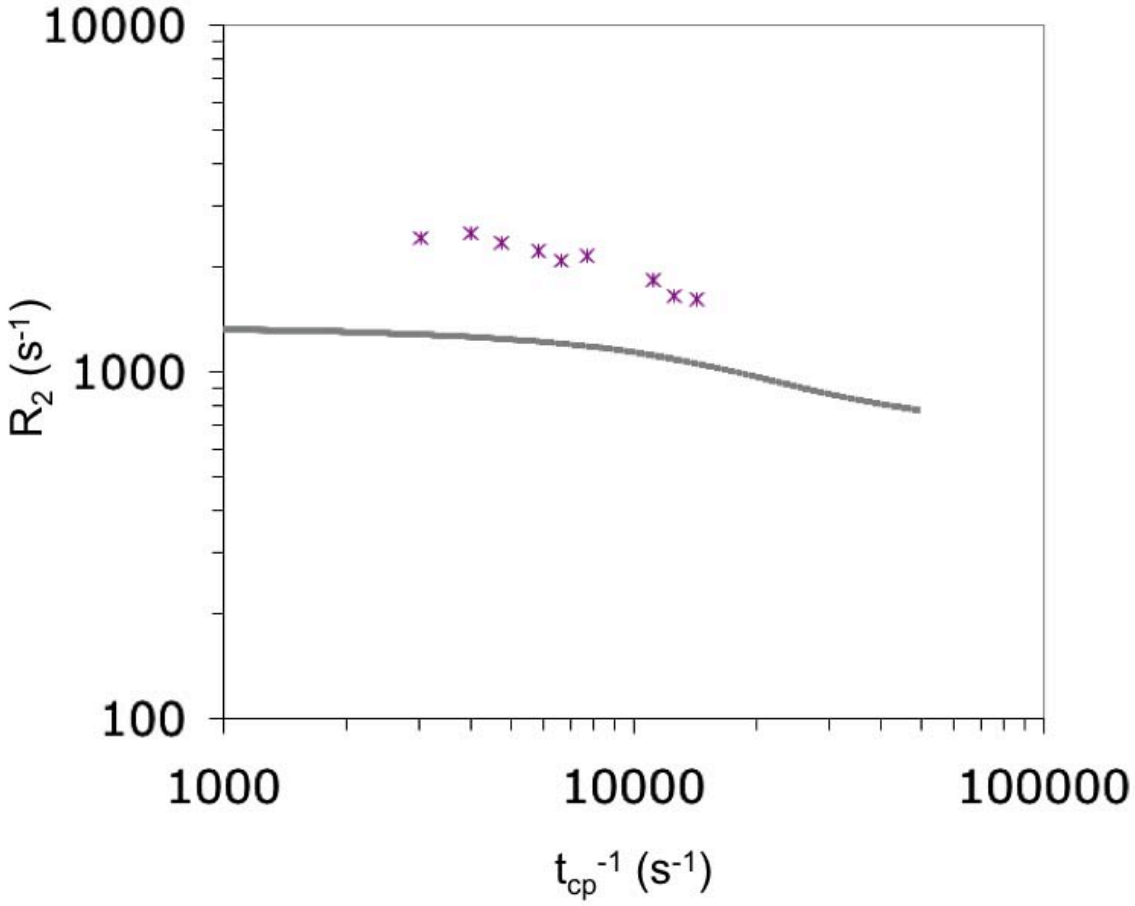

Figure 11: Model Log-Log plot of R2 vs. 1/tcp Calculated From 13C NMR Lineshape Fit. Experimental data for the saturated surface is also shown.

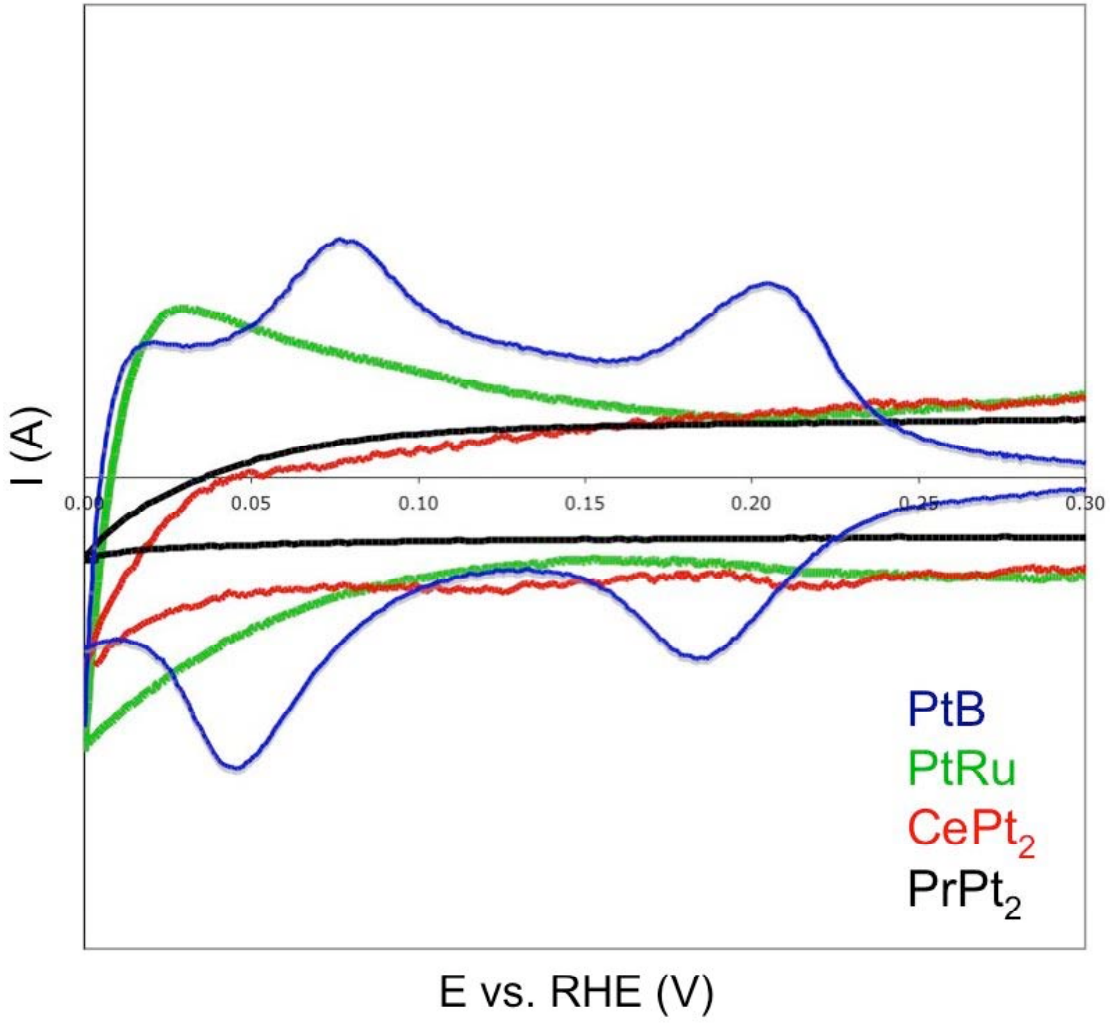

Figure 12. “Hydrogen region” of clean Pt black, PtRu black, and platinum lanthanide alloys. The anodic and cathodic currents only show structure for the case of pure platinum.

Publications and Reports Supported under this Contract

Papers published in peer-reviewed journals

Patrick McGrath, Aurora Marie Fojas, Benjamin Rush, Jeffrey A. Reimer, Elton J. Cairns, Characterizing electrocatalytic surfaces: Electrochemical and NMR studies of methanol and carbon monoxide on Pt/C, *Electrochim. Acta* **53**, 1365–1371 (2007)

Patrick McGrath, Aurora Marie Fojas, Jeffrey A. Reimer, and Elton J. Cairns, "Site-dependent ^{13}C chemical shifts of CO adsorbed on Pt electrocatalysts", J. Phys. Chem.C, **112**, 14702–14705. **(**2008**)**

Patrick McGrath, Aurora Marie Fojas, Jeffrey A. Reimer, and Elton J. Cairns, "Electro-oxidation Kinetics of Adsorbed CO on Platinum Electrocatalysts", Chemical Engineering Science, In Press.

Papers presented at meetings

Aurora Marie Fojas, Patrick McGrath, Elton J. Cairns, Jeffrey A. Reimer. *Characterization of Electro-oxidation Catalysts fro Alcohol-Powered Fuel Cells*, Rocky Mountain Conference on Analytical Chemistry, Denver, CO. Aug., 2005

A.M. Fojas, P. McGrath, A. Deb, K. Lux, E. J. Cairns, and J. Reimer, "Design Of Novel Fuel Cell Electrocatalysts: Probing Electronic and Geometric Structure", Presented at the Electrochemical Society Meeting, Los Angeles, Oct. 16-21, 2005

Patrick McGrath, Aurora Marie Fojas, Benjamin Rush, Kenneth Lux, Elton Cairns, and Jeffrey Reimer. *Combined Electrochemical and NMR Studies of the Electrocatalytic Interface for Direct Alcohol Fuel Cells*. Experimental Nuclear Magnetic Resonance Conference, Asilomar, CA.. April, 2006

Patrick McGrath, Aurora Marie Fojas, Benjamin Rush, Jeffrey A. Reimer, and Elton J. Cairns, Combined Voltammetric and ^{13}C NMR Study of Methanol on Pt/C Electrocatalyst, Presented at The Electrochemical Society Meeting, Denver, CO, May 8-12, 2006

Patrick McGrath, Aurora Marie Fojas, Benjamin Rush, Elton Cairns and Jeffrey Reimer, Site-Dependent Knight Shift of Electrochemically Adsorbed ^{13}CO on Pt-Nanoparticles, , Presented at the Rocky Mountain Conference, Colorado, June, 2006

Patrick McGrath, Aurora Marie Fojas, Benjamin Rush, Elton Cairns, Jeffrey Reimer. *Site-Dependent Knight Shift of Chemically Adsorbed ^{13}CO on Pt-Nanoparticles*. Rocky Mountain Conference on Analytical Chemistry, Breckinridge, CO, July, 2006

A.M. Fojas, P. McGrath, J. A. Reimer, E. J. Cairns, Characterizing Novel Electrocatalytic Surfaces: Combined Electrochemical and Nuclear Magnetic Resonance Studies, Presented at the International Society of Electrochemistry Meeting, Edinburgh, Scotland, August 27, 2006

Patrick McGrath, Aurora Marie Fojas, Benjamin Rush, Jeffrey A. Reimer, and Elton J. Cairns, Combined Voltammetric and ^{13}C NMR Study of Methanol on Pt/C Electrocatalyst, Presented at Yonsei University, Seoul, Korea, May 30. 2007

P. McGrath, A.M. Fojas, J.A. Reimer, and E.J. Cairns, CO Oxidation from Fuel Cell Catalysts: A Combined Electrochemical and Spectroscopic Study, Presented at the Electochemical Society Meeting, Washington, DC, Oct., 2007

P. McGrath, A.M. Fojas, E. J. Cairns, and J. Reimer, Surface Site Characterization of CO_{ads} on Platinum, Presented at the American Physical Society Meeting, New Orleans, March, 2008

Elton J. Cairns, Surface Site Characterization of CO*ads* on Platinum Fuel Cell Electrocatalysts, Invited Lecture at Hyundai Motor Corp, Swindon, Korea, May 23, 2008

Elton J. Cairns, Surface Site Characterization of CO*ads* on Platinum Fuel Cell Electrocatalysts, Presented to Korea Energy Inst., Seoul, Korea, May 27, 2008

P. McGrath, A.M. Fojas, J. A. Reimer, and E. J. Cairns, Adsorbate Characterization on DAFC Electrocatalysts, presented at the ISE Meeting, Seville, Sept., 2008

Aurora Marie Fojas, Patrick McGrath, Jeffrey A. Reimer, and Elton J. Cairns, CO Mobility on Pt Electrocatalysts: An NMR Study, Presented at The Electrochemical Society Meeting, San Francisco, May 25-30, 2009

Technical reports submitted to ARO

Elton J. Cairns and Jeffrey A. Reimer, New Electrocatalysts for Direct Oxidation of Organic Fuels, Army Research Office Interim Progress Report, August 14, 2006

Elton J. Cairns and Jeffrey A. Reimer, New Electrocatalysts for Direct Oxidation of Organic Fuels, Army Research Office Interim Progress Report for August 1, 2006- July 31, 2007

Participating Scientific Personnel

Patrick McGrath: earned MS and PhD degrees

Aurora Marie Fojas: earned MS and PhD degrees

Bong-Ok Park, visiting researcher, electrocatalyst synthesis and characterization

Rossana Chen, undergraduate student, electrocatalyst synthesis

Stephanie Didas, undergraduate student, NMR

Bibliography

1. B. McNicol, D. Rand, K. Williams *J. Power Sources.* (1999), 83, 15.

2. R. Dillon, S. Srinivasan, A. Aricò, V. Antonucci. *J. Power Sources*. (2004), 127, 112.

3. A.V. Tripkovic, K.D.Popovic, B.N. Grgur, B.Blizanac, P.N. Ross, N.M. Markovic, *Electrochimica Acta*, (2002), 47, 3707-3714.

4. F. Seland, R. Tunold, D.A. Harrington, *Electrochimica Acta*, (2006), 51 3827-3840.

5. H. Gasteiger, N. Markovic, P. Ross, Jr., E. Cairns. *J. Phys. Chem.* (1993), 97, 12020.

6. H. Gasteiger, N. Markovic, P. Ross, Jr., E. Cairns. *J. Electrochem. Soc*. (1994), 141, 1795.

7. H. Gasteiger, N. Markovic, P. Ross, Jr., E. Cairns *Electrochimica Acta*, (1994), 39, 1825.

8. K. Lux. *PhD Dissertation, Univ. of California, Berkeley*, 2003.

9. A.M. Fojas. *M.S. Thesis, University of California Berkeley*, 2004.

10. K. Lux, E. Cairns. *J. Electrochem. Soc. (*2006), 153, A1132.

11. N.M. Markovic, P.N. Ross, *Surf. Sci. Rep*., (2002),45, 117-229.

12. S. Park, Y.Y. Tong, A. Wieckowski, E. Oldfield, M.J. Weaver, *Langmuir*, (2002), 18, 3233-3240.

13. N.P. Lebedeva, A Rodes, J.M. Felin, M.T.M. Koper, R.A. van Santen, *J. Phys. Chem. B* (2002), 106, 9863-9872.

14. F. Vidal, B. Bussou, A. Tadjeddine, *Electrochimica Acta*, (2004), 49, 3637-3641.

15. F. Maillard, E.R. Savinova, P.A. Simonov, V.I. Zaikovski, U. Stimming, *J. Phys. Chem. B*, (2004), 108, 17893-17904.

16. Z-Y. Zhou, N. Tian, Y-J. Chen, S-P. Chen, S-G. Sun, *J. Electroanal. Chem*.,(2004), 573, 111-119

17. Y.G. Yan, Q.X. Li, S.J. Huo, M. Ma, W.B. Cai, M. Osawa, *J. Phys. Chem. B*, (2005), 109, 7900-7906.

18. M. Arenz, K. Mayrhofer, V. Stamenkovic, B. Blizanac, T. Tomoyuki, P.N. Ross, N.M. Markovic, *J. Am. Chem. Soc*., (2005), 127, 6819-6829.

19. H. Rhodes, P. Wang, H. Stokes, C. Slichter, J. Sinfelt. *Phys. Rev. B.*, (1982), 26, 3559.
20. J. van der Klink, J. Buttet, M. Graetzel. *Phys. Rev. B*. (1984), 29, 11.

21. C. Makowka, C. Slichter, J. Sinfelt. *Phys. Rev. B*. (1985), 31, 5663.

22. A. Clogston, V. Jaccarino, Y. Yafer. *Phys. Rev.* (1964), 134, A650.

23. R. Watson, A. Freeman. *Phys. Rev*. (1961), 123, 2027.

24. Y.Y. Tong, C. Rice, N. Godbout, A. Wieckowski, E. Oldfield. *J. Am. Chem. Soc.* (1999), 121, 2996.

25. Y.Y. Tong, C. Rice, A. Wieckowski, E. Oldfield *J. Am. Chem. Soc*. 2000, 122, 11921.
26. V. Compton, B. Matthias. *Acta Cryst*. (1959), 12, 651.

27. K. Aoki, T. Yamamoto, T. Masumoto. *Scripta Metallurgica*. (1987), 21, 27.

28. M. Yahnke, B. Rush, J. Reimer, E. Cairns. *J. Am. Chem. Soc*. (1996), 118, 12250.

29. B. Rush, J. Reimer, E. Cairns. *J. Electrochem. Soc. (*2001), 148, A137.

30. Elton J. Cairns and Jeffrey A. Reimer, "New Electrocatalysts for Direct Oxidation of Organic Fuels", ARO Interim Progress Report 1, Project 48713-CH, August 14, 2006

31. Patrick McGrath, Aurora Marie Fojas, Benjamin Rush, Jeffrey A. Reimer, Elton J. Cairns, Characterizing electrocatalytic surfaces: Electrochemical and NMR studies of methanol and carbon monoxide on Pt/C, *Electrochim. Acta*, (2007), **53**, 1365–1371

32. Kenneth W. Lux and Elton J. Cairns, "Lanthanide-Platinum Intermetallic Compounds as Anode Electrocatalysts for Direct Ethanol PEM Fuel Cells I. Synthesis and Characterization of LnPt2 (Ln = Ce,Pr) Nanopowders", *Journal of The Electrochemical Society*, 153, 6, A1132-A1138 (2006)

33. Patrick McGrath, Aurora Marie Fojas, Jeffrey A. Reimer, and Elton J. Cairns, "Electro-oxidation Kinetics of Adsorbed CO on Platinum Electrocatalysts", Chemical Engineering Science, in press.

34. Elton J. Cairns and Jeffrey A. Reimer, "New Electrocatalysts for Direct Oxidation of Organic Fuels", ARO Interim Progress Report 2, Project 48713-CH, August 20, 2007

35. Patrick McGrath, Aurora Marie Fojas, Jeffrey A. Reimer, and Elton J. Cairns, "Site-

dependent ^{13}C chemical shifts of CO adsorbed on Pt electrocatalysts", *J. Phys. Chem.C,* **(**2008**), 112**, 14702–14705.

36. H. Gutowsky, R. Vold, E. Wells, "Theory of Chemical Exchange Effects in Magnetic Resonance," *J.Chem.Phys*., (1965), 43, 4107.

37. A. Allerhand, H. Gutowsky, "Spin-Echo Studies of Chemical Exchange," *J.Chem.Phys.,(*1965), 42, 1587.

38. J. Carver, R. Richards, "A General Two-Site Solution for the Chemical Excahnge Produced Dependence of T2 Upon the Carr-Purcell Pulse Separation," *J.Mag.Res.,* (1972), 6, 89.

39. J. Jen, "Chemcial Exchange and NMR T2 Relaxation - The Multisite Case," *J.Mag.Res.,* (1978), 30, 111.

40. W. Sobel, "A Complete Solution to the Model Describing Carr-Purcell and Carr-Purcell-Meiboom-Gill Experiemnts in a Two-Site Exchange System," *Mag.Res.Med.* (1991), 21, 2.

41. D. Davis, M. Perlman, R. London, "Direct Measurements of the Dissociation-Rate Constant for Inhibitor-Enzyme Complexes via the T1 and T2 (CPMG) Methods," *J.Mag.Res.B*, (1994), 104, 266.

42. A. Palmer, "NMR Characterization of Dynamics of Biomacromolecules," *Chem.Rev*., (2004), 104, 3623.

43. D. Abergel, A. Palmer, "Approximate Solutions of the Bloch-McConnell Equations for Two-Site Chemical Exchange," *Chem.Phys.Chem.*, (2007), 5, 787.

44. M. Cuperlovic, G. Meresi, W. Palke, J. Gerig, "Spin Relaxation and Chemical Exchange in NMR Simulations," *J.Mag.Res*., (2000), 142, 11.

45. B. Rush, Chemical Engineering Doctoral Dissertation. University of California, Berkeley.1999.

46. P. Mcgrath. Chemical Engineering Doctoral Dissertation. University of California, Berkeley. 2007.

47. M. Yahnke, Chemical Engineering Masters Dissertation. University of California, Berkeley. 1996.

48. Aurora Marie Fojas, PhD Dissertation, University of California, Berkeley, 2008.

49. M. Levitt. Spin Dynamics: Basics of Nuclear Magnetic Resonance. Wiley and Sons., New York, 2002.

50. J. Ansermet, PhD Thesis, University of Illinois (1985).

51. K. Zilm, L. Bonneviot, D. Hamilton, G. Webb, G. Haller, “Carbon-13 NMR Studies of CO Adsorbed on Supported Platinum and Palladium Catalysts Using Magic Angle Spinning,” *J.Phys.Chem.B,* (1990), 94, 1463.

52. J. Ansermet, C. Slichter, J. Sinfelt, “An NMR study of the geometry of a CO layer chemisorbed on Pt particles,” J.Chem.Phys., 88 (1988) 5963

53. J. Day, P. Vuissoz, E. Oldfield, A. Wieckowski, J. Ansermet, “Nuclear Magnetic Resonance Spectroscopic Study of the Electrochemical Oxidation Product of Methanol on Platinum Black,” *J.A.C.S.,* (1996), 118, 13046.